IEEE Access
Multidisciplinary | Rapid Review | Open Access Journal

Received November 19, 2019, accepted December 12, 2019, date of publication December 17, 2019,
date of current version December 31, 2019.

Digital Object Identifier 10.1109/ACCESS.2019.2960327

Periodic Topology Optimization of a Stacker Crane

HONG-YU JIAO[1,2,3], FENG LI[1], ZHENG-YI JIANG[3], YING LI[2], AND ZHAO-PENG YU[2]

[1]Suzhou Institute of Nano-Tech and Nano-Bionics (SINANO), Chinese Academy of Sciences, Suzhou 215000, China
[2]School of Automotive Engineering, Changshu Institute of Technology, Suzhou 215500, China
[3]School of Mechanical, Materials, Mechatronic and Biomedical Engineering, University of Wollongong, Wollongong, NSW 2519, Australia

Corresponding author: Zhao-Peng Yu (yuzhaopeng@cslg.edu.cn)

This work was supported in part by the National Natural Science Foundation of China under Grant 51605046, and in part by the Jiangsu Provincial Government Scholarship Program under Grant JS-2017-188.

ABSTRACT The stacker crane is a long-and-thin structure with a large length-to-width ratio. It is difficult to obtain a topology configuration with good period properties using traditional optimization methods. While the mathematical model of periodic topology optimization—in which the elements' relative densities are selected as design variables, and mean compliance as the objective function—is established. To find a topology configuration with a good period property, an additional constraint condition must be imported into the mathematical model. According to the optimization criteria method, the iterative formula of design variables is derived in the virtual sub domain. To verify the capability and availability of the proposed method, periodic topology optimization of a single-mast stacker crane is investigated in this paper. The results show that configurations with good periodicity can be obtained when the number of sub domains is varied. After considering mean compliance and complexity, the optimal configuration has eight periods. A preliminary lightweight design scheme is proposed based on this configuration of a stacker crane, which is a periodic feature structure.

INDEX TERMS Periodic topology optimization, long-and-thin structures, stacker crane, variable density method, optimization criteria method.

I. INTRODUCTION

An effective design tool, structural topology optimization, can obtain a lighter structure than size and shape optimization, and it has broad application prospects with regard to the lightweight design of engineering structures [1]–[4]. There have been many topology optimization methods presented, including the homogenization method [5], [6], variable density method [7], [8], level set method [9], [10], evolutionary structural optimization method [11], [12], phase field method [13], [14], independent continuous mapping method [15], [16] and topological derivative method [17]. Many international research studies have been carried out on this topic. Yuanfang *et al.* [18] used topology optimization to study a mini-electrical vehicle frame. Considering the impact loads under multiple working conditions, a new structure was proposed using the variable density method to meet layout and real driving demands. The new structure is rational and can reduce the weight of the mini-electrical vehicle frame and improve mechanical performance. The modified P-norm correction method proposed by Lee et al. was used to present maximum stress-constrained structural optimization based on the phase field design method [19]. To overcome the limitation of conventional P-norm methods, the lower-bound P-norm stress curve was employed. Lightweight designs for the L-shaped and cantilever beams were proposed for the verification of the proposed method under the condition of yield strength constraint. The level set-based topology optimization method proposed by Wang and Kang [9] was used to study the design of structures with coating layers. The optimization problem of compliance minimization was considered with a material mass constraint. To solve the optimization problem, the steepest descent method was used. Some examples in both 2D and 3D designable domains were researched to show the effectiveness of the proposed method. The variable density method, phase field design method, and level set method can be used to research the topology optimization of engineering structures. However, topology configurations with periodicity are not obtained through these traditional methods.

Periodic feature structures have attracted the attention of academic and industrial technicians with their unique structural form, excellent visual aesthetics, extensibility in array

The associate editor coordinating the review of this manuscript and approving it for publication was Wei Wei.

direction, physical versatility, and good manufacturing and design [20]–[25]. Many topology optimization methods have been presented to research periodic topology optimization, including the homogenization method, evolutionary structural optimization method [26]–[29], and independent continuous mapping method [30], [31]. Huang and Xie [26] used bidirectional evolutionary structural optimization to research the topology optimization of periodic structures and presented a new method. This method is widely applied to structural periodic topology optimization problems on cyclic-symmetry structures [27], natural frequencies [28] and unstructured design points [29]. The topology optimization model of the periodic structures was established by Long and Jia using the solid isotropic material with penalization (SIMP) method and the independent continuous mapping (ICM) method. This model is used to optimize the optimal topological configuration for thermal conductive microstructures of composite materials [30], [31]. The stacker crane is considered a long-and-thin structure because it has a large length-to-width ratio. It is often difficult to obtain a topology configuration with a good period property by traditional topology optimization methods. The abovementioned studies provide an important basis and reference for the topology optimization of stacker cranes.

The paper is structured as follows. First, in the second section, we introduce the problem description of periodic topology optimization and the material interpolation model. In the third section, the mathematical model of periodic topology optimization is established. The iterative formula of the virtual sub domain can be obtained based on the optimization criteria method. Section 4 presents the filter function and convergence criterion. Section 5 studies finite element analysis of a single-mast stacker crane. To verify the capability and availability of the proposed method, periodic topology optimization of stacker cranes is investigated in section 6. A preliminary lightweight design scheme is proposed in section 7. Final conclusions are drawn in section 8.

II. LONG-AND-THIN STRUCTURES FOR PERIODIC DESIGN

A. PROBLEM DESCRIPTION OF PERIODIC TOPOLOGY OPTIMIZATION

The objective of periodic topology optimization is to seek an optimal topology configuration with good period properties. To consider the periodicity of long-and-thin structures in a given design domain, the design domain is divided into m sub domains on the length direction, where m denotes the number of sub domains along direction x, as shown in Fig. 1. The number of sub domains is usually prescribed according to the length-to-width ratio of long-and-thin structures. The conventional topology optimization is considered periodic topology optimization for $m = 1$. $x_{i,j}$ is the design variable, where i denotes the sub domain number, and j denotes the element number in a sub domain.

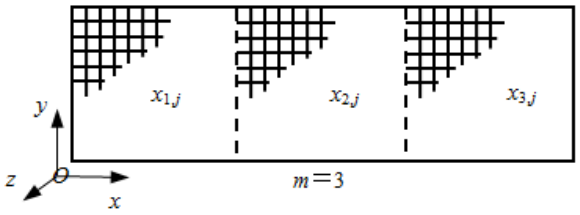

FIGURE 1. Design domain with m=3 sub domains.

B. MATERIAL INTERPOLATION MODEL IN THE VARIABLE DENSITY METHOD

SIMP is one of the most popular material interpolation methods and was first considered by Bendsøe in 1989. This interpolation model is referred to as the power law or penalized, proportional stiffness model [32]. In this paper, the relationship between the modulus of elasticity after interpolation and relative density is expressed as:

$$E(x_{i,j}) = E_{\min} + (x_{i,j})^p (E_0 - E_{\min}) \tag{1}$$

where $E(x_{i,j})$ is the modulus of elasticity after interpolation, E_0 is the modulus of elasticity of the material, $E_{\min}$ is usually restricted to $0.001^* E_0$ for the numerical stability, $x_{i,j}$ is the relative density of the jth element in the ith sub domain, and p is the penalization factor.

III. SOLVING THE PROBLEM OF PERIODIC TOPOLOGY OPTIMIZATION

A. MATHEMATICAL MODEL OF PERIODIC TOPOLOGY OPTIMIZATION

The objective function of periodic topology optimization is to minimize the mean compliance of long-and-thin structures subjected to volume constraints and other factors. The elements' relative densities are selected as design variables. Based on the variable density method, the mathematical model of periodic topology optimization can be written as:

$$\begin{aligned}
&\text{Find } \boldsymbol{X} = (x_{1,1}, x_{1,2}, x_{1,3}, \ldots, x_{i,j})^{\mathrm{T}} \in \mathbf{R} \\
&\qquad i = 1, 2, \cdots, m, \quad j = 1, 2, \cdots, n \\
&\text{Min } C(\boldsymbol{X}) = \frac{1}{2}\boldsymbol{F}^{\mathrm{T}}\boldsymbol{U} = \frac{1}{2}\boldsymbol{U}^{\mathrm{T}}\boldsymbol{K}\boldsymbol{U} \\
&\qquad = \frac{1}{2}\sum_{i=1}^{m}\sum_{j=1}^{n}\boldsymbol{u}_{i,j}^{\mathrm{T}}\boldsymbol{k}_{i,j}\boldsymbol{u}_{i,j} = \frac{1}{2}\sum_{i=1}^{m}\sum_{j=1}^{n}\left(x_{i,j}\right)^p \boldsymbol{u}_{i,j}^{\mathrm{T}}\boldsymbol{k}_0\boldsymbol{u}_{i,j} \\
&\text{s.t } \boldsymbol{K}\boldsymbol{U} = \boldsymbol{F} \\
&\qquad V = f \cdot V_0 = \sum_{i=1}^{m}\sum_{j=1}^{n} x_{i,j} \cdot v_{i,j} \\
&\qquad x_{1,j} = \cdots = x_{i,j} = \cdots x_{m,j} \\
&\qquad 0 < x_{\min} \le x_{i,j} \le x_{\max} \le 1
\end{aligned} \tag{2}$$

where C is the mean compliance; $\boldsymbol{U}$ and $\boldsymbol{F}$ are the displacement vectors and applied load, respectively; $\boldsymbol{K}$ is the total stiffness matrix; $v_{i,j}$ and $\boldsymbol{k}_{i,j}$ are the volume and the stiffness matrix, respectively, of the jth element in the ith sub domain; $\boldsymbol{u}_{i,j}$ is the nodal displacement vector of the jth element in

the ith sub domain; and $x_{\max}$ and $x_{\min}$ are the maximum and minimum relative density of elements, respectively.

To make each sub domain have a periodic topology configuration, a constraint condition is set up in the mathematical model, which is expressed as:

$$x_{1,j} = \cdots = x_{i,j} = \cdots x_{m,j} \tag{3}$$

The solution method of topology optimization is generally divided into two categories: the mathematical programming method [33], [34] and the optimization criteria method [35], [36]. The mathematical programming method is highly versatile and can be applied to different optimization problems. However, the number of iterations is large, and the solution efficiency is not high. The outstanding advantage of the optimization criteria method is that the convergence speed is fast, the number of iterations is small, and it has nothing to do with the size and complexity of the structure. The topology optimization problem with simple constraints and a large number of optimization variables has higher efficiency. Due to the above advantages, the optimization criteria method is selected as the solution method of periodic topology optimization.

B. OPTIMIZATION CRITERIA METHOD FOR PERIODIC TOPOLOGY OPTIMIZATION

The optimization criteria formula, which consists of an objective function and constraint conditions, can be derived from the Lagrange function [37]. The Lagrange function of the periodic topology optimization problem can be written as:

$$\begin{aligned} L = {} & C + \lambda_1 (V - f \cdot V_0) + \boldsymbol{\lambda}_2^{\mathrm{T}} (\boldsymbol{KU} - \boldsymbol{F}) \\ & + \sum_{i=1}^{m} \sum_{j=1}^{n} \lambda_{3i,j} (x_{\min} - x_{i,j} + a_{i,j}^2) \\ & + \sum_{i=1}^{m} \sum_{j=1}^{n} \lambda_{4i,j} (x_{i,j} - x_{\max} + b_{i,j}^2) + \sum_{i=1}^{m-1} \beta_i \left(x_{i,j} - x_{i+1,j}\right) \end{aligned} \tag{4}$$

where $\lambda_1, \boldsymbol{\lambda}_2, \lambda_{3i,j}, \lambda_{4i,j}, \beta_i$ are Lagrange multipliers; λ_1, $\lambda_{3i,j}$, $\lambda_{4i,j}$, β_i are scalars; $\boldsymbol{\lambda}_2$ is a column vector; and $a_{i,j}^2$ and $b_{i,j}^2$ are relaxation factors.

When $x_{i,j}$ is taken as the extreme value $x_{i,j}^*$, the Lagrange function should satisfy the following Kuhn-Tucker conditions:

$$\begin{cases} \dfrac{\partial L}{\partial x_{i,j}} = \dfrac{\partial C}{\partial x_{i,j}} + \lambda_1 \dfrac{\partial V}{\partial x_{i,j}} + \boldsymbol{\lambda}_2^{\mathrm{T}} \dfrac{\partial (\boldsymbol{KU})}{x_{i,j}} - \lambda_{3i,j} + \lambda_{4i,j} = 0 \\ V = f \cdot V_0 \\ \boldsymbol{F} = \boldsymbol{KU} \\ \lambda_{3i,j} \left(x_{\min} - x_{i,j}\right) = 0 \quad i = 1, 2, \cdots, m \\ \lambda_{4i,j} \left(x_{i,j} - x_{\max}\right) = 0 \quad j = 1, 2, \cdots, n \\ \lambda_{3i,j} > 0 \\ \lambda_{4i,j} > 0 \\ x_{\min} \le x_{i,j} \le x_{\max} \end{cases} \tag{5}$$

If $x_{\min} < x_{i,j} < x_{\max}$, then:

$$\frac{\partial L}{\partial x_{i,j}} = \frac{\partial C}{\partial x_{i,j}} + \lambda_1 \frac{\partial V}{\partial x_{i,j}} + \boldsymbol{\lambda}_2^{\mathrm{T}} \frac{\partial (\boldsymbol{KU})}{\partial x_{i,j}} = 0 \tag{6}$$

When the equation $C = {}^1\!/_2 \boldsymbol{U}^{\mathrm{T}} \boldsymbol{KU}$ is plugged into Eq.6, the following can be obtained:

$$\begin{aligned} \frac{\partial L}{\partial x_{i,j}} = {} & \frac{1}{2} \left(\frac{\partial \boldsymbol{U}^{\mathrm{T}}}{\partial x_{i,j}} \boldsymbol{KU} + \boldsymbol{U}^{\mathrm{T}} \frac{\partial \boldsymbol{K}}{\partial x_{i,j}} \boldsymbol{U} + \boldsymbol{U}^{\mathrm{T}} \boldsymbol{K} \frac{\partial \boldsymbol{U}}{\partial x_{i,j}} \right) \\ & + \lambda_1 \frac{\partial V}{\partial x_{i,j}} + \boldsymbol{\lambda}_2^{\mathrm{T}} \left(\frac{\partial \boldsymbol{K}}{\partial x_{i,j}} \boldsymbol{U} + \boldsymbol{K} \frac{\partial \boldsymbol{U}}{\partial x_{i,j}} \right) = 0 \end{aligned} \tag{7}$$

Using the symmetry of the stiffness matrix, Eq. 7 can be written as:

$$\begin{aligned} \frac{\partial L}{\partial x_{i,j}} = {} & (\boldsymbol{\lambda}_2^{\mathrm{T}} \boldsymbol{K} + \boldsymbol{U}^{\mathrm{T}} \boldsymbol{K}) \frac{\partial \boldsymbol{U}}{\partial x_{i,j}} + \lambda_1 \frac{\partial V}{\partial x_{i,j}} \\ & + \left(\frac{1}{2} \boldsymbol{U}^{\mathrm{T}} + \boldsymbol{\lambda}_2^{\mathrm{T}} \right) \frac{\partial \boldsymbol{K}}{\partial x_{i,j}} \boldsymbol{U} = 0 \end{aligned} \tag{8}$$

If λ_2 is a column vector and its value is no limit. The equation $\lambda_2 = -\boldsymbol{U}$ is substituted with Eq.8, and then the following can be obtained:

$$\frac{\partial L}{\partial x_{i,j}} = -\frac{1}{2} \boldsymbol{U}^{\mathrm{T}} \frac{\partial \boldsymbol{K}}{\partial x_{i,j}} \boldsymbol{U} + \lambda_1 \frac{\partial V}{\partial x_{i,j}} = 0 \tag{9}$$

When the equations $k_{i,j} = (x_{i,j})^p k_0$ and $V = \sum_{i=1}^{m} \sum_{j=1}^{n} x_{i,j} v_{i,j}$ are plugged into Eq.9, then:

$$-\frac{p}{2} (x_{i,j})^{p1} \boldsymbol{u}_{i,j}^{\mathrm{T}} \boldsymbol{k}_0 \boldsymbol{u}_{i,j} + \lambda_1 v_{i,j} = 0 \tag{10}$$

Usually, the design domain is divided into several elements in which the element size is identical. Thus, element volume $v_{i,j}$ in the design domain is given by:

$$v_{i,j} = v_0 \tag{11}$$

where v_0 is the volume of finite element mesh.

Then, multiply both sides by $x_{i,j}/p$:

$$\frac{1}{2} \boldsymbol{u}_{i,j}^{\mathrm{T}} \boldsymbol{k}_{i,j} \boldsymbol{u}_{i,j} = \frac{\lambda_1 v_0}{p} \times x_{i,j} \tag{12}$$

The strain energy of the jth element in the ith sub domain is calculated by:

$$c_{i,j} = \frac{1}{2} \boldsymbol{u}_{i,j}^{\mathrm{T}} \boldsymbol{k}_{i,j} \boldsymbol{u}_{i,j} \tag{13}$$

Then, Eq. 12 is expressed as:

$$c_{i,j} = \frac{\lambda_1 v_0}{p} \times x_{i,j} \tag{14}$$

Eq.14 applies to all elements in the design domain. Its physical meaning is that the relative density is proportional to the strain energy of the element. It is easy to find that both sides of Eq.14 are summed simultaneously, and then

$$\sum_{i=1}^{m} c_{i,j} = \frac{\lambda_1 v_0}{p} \times \sum_{i=1}^{m} x_{i,j} \tag{15}$$

A virtual sub domain is constructed, and the size, number, and distribution of elements in the virtual sub domain must be identical to each sub domain. The average strain energy of elements in all sub domains is taken as the strain energy of elements in the virtual sub domain, which can be formulated as follows:

$$c_j = \frac{1}{m}\sum_{i=1}^{m} c_{i,j} \tag{16}$$

To obtain an optimal periodic topology, a constraint condition is set up. This means that the average relative density of the jth element in all sub domains is calculated as:

$$x_j = \frac{1}{m}\sum_{i=1}^{m} x_{i,j} = x_{i,j} \tag{17}$$

If we put Eq. 16 and Eq. 17 into Eq. 15, we obtain the following:

$$c_j = \frac{\lambda_1 v_0}{p} \times x_j \tag{18}$$

The physical meaning of Eq. 18 is that the relative density is proportional to the strain energy of elements in the virtual sub domain. It is expressed in another form as:

$$D_j^{(k)} = \frac{pc_j}{\lambda_1 v_0 x_j} = 1 \tag{19}$$

The iterative formula of the virtual sub domain based on the optimality criterion method can be obtained, as follows:

$$x_j^{(k+1)} = \begin{cases} \left[D_j^{(k)}\right]^{\eta} x_j^{(k)} & x_{\min} < \left[D_j^{(k)}\right]^{\eta} x_j^{(k)} < x_{\max} \\ x_{\min} & \left[D_j^{(k)}\right]^{\eta} x_j^{(k)} \le x_{\min} \\ x_{\max} & \left[D_j^{(k)}\right]^{\eta} x_j^{(k)} \ge x_{\max} \end{cases} \tag{20}$$

where η is the damping coefficient. It is generally taken as 0.5. The aim of introducing η is to ensure that optimization results are convergent.

IV. FILTER FUNCTION AND CONVERGENCE CRITERION

A. FILTER FUNCTION

Due to the instability of numerical calculations, checkerboard patterns are often observed in the topology optimization process. A filter function proposed by Sigmund and Petersson in 1998 is imported to solve these checkerboard and mesh-independent problems [38]. Huang and Xie [39] studied convergent and mesh-independent solutions for the BESO method. A mesh-independency filter function was introduced into BESO to determine the addition of elements and to eliminate unnecessary structural details below a certain length scale in the design. Based on the filtration scheme in reference [39], an improved filtration scheme was proposed based on the element strain energy.

The zone Ω_a denotes an open ball centered on element a and with a radius of $r_{\min}$. We note that all elements in the zone are used to calculate the strain energy of element a after filtering:

$$c_a' = \frac{\sum_{e=1}^{l} d_e c_e}{\sum_{e=1}^{l} d_e} \tag{21}$$

where c_a' is the strain energy of element a after filtering; c_e is the strain energy of element e before filtering, which is $c_{i,j}$ in Eqs. 13∼16 replacing the subscript symbol because i is the sub domain number, and its value is $i = 1, 2, \ldots, m$; j is the element number in a sub domain, and its value is $j = 1, 2, \ldots, n$. There are $N = m \times n$ elements in the entire optimization domain. The strain energy of all the elements in the entire optimization domain can be filtered as a whole, and it is not necessary to distinguish each sub domain. Thus, the subscript of the element strain energy symbol is replaced in Eq. 21. l is the element number in zone Ω_a. d_e is the weight coefficient:

$$d_e = r_{\min} - r_{ea} \tag{22}$$

where r_{ea} is the distance from the center of each element in the zone to the center of element a.

B. CONVERGENCE CRITERION

It is well known that if the relative error τ of the two adjacent optimization results is less than the given convergence accuracy $\tau_{\max} = 0.001$, then the periodic layout optimization has converged. The mean compliance is selected as the objective function of periodic topology optimization. The relative change in the objective function is regarded as the convergence criterion. It can be formulated as follows:

$$\tau = \frac{\left|\sum_{k=1}^{N} (C^k - C^{k-1})\right|}{\sum_{k=1}^{N} C^{k-1}} \le \tau_{\max} \tag{23}$$

In the optimization process, the relative error τ of the two adjacent optimization results must be calculated. When the convergence criterion shown in Eq.23 is satisfied, we propose that $x_{i,j}$ is taken as the extreme value $x_{i,j}^*$.

V. FINITE ELEMENT ANALYSIS OF A SINGLE-MAST STACKER CRANE

A. THE MECHANICAL MODEL OF A SINGLE-MAST STACKER CRANE

Single-mast stacker cranes are in their worst condition when the pallet is fully loaded and extended to the highest position. If a single-mast stacker crane is simplified as the mast and bottom end rail. Other parts are equivalent to forces in the mechanical model [40]–[42] shown in Fig. 2, as follows: H and B are the height and wheel track of the stacker crane, and P_{H} is a horizontal inertia force. When the stacker crane is in a condition of rest, the value of P_{H} is zero; h is the distance

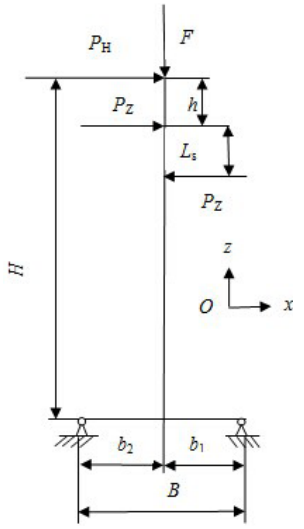

FIGURE 2. Mechanical model of a single-mast stacker crane.

of top contact roller and the top of mast; b_1 and b_2 are the distance of the neutral axis of the mast cross section and two fulcrums of the bottom end rail, respectively; F is an axial force on the top of the mast; and P_z is a horizontal force between the mast and rollers.

B. FINITE ELEMENT MODEL OF A STACKER CRANE

Our research object is a single-mast stacker crane with a 1-ton lifting capacity Q and 8 meters of lifting height H. The mast and bottom end rail are welded with several pieces of steel plate of different thicknesses. The mast and bottom end rail are simulated with shell element 63 for different thicknesses, and the material is steel Q235B. The guide rail adopts 60×40 square steel from steel Q345. The guide rail is simulated with beam element 188. The finite element model of a stacker crane is established in ANSYS shown in Fig. 3.

The constraints and loads are applied to the finite element model according to the mechanical model shown in Fig. 2. The bottom end rail is studied as simply a supported beam. The most dangerous condition is when the pallet is fully loaded at the highest position. In this case, the force condition of the mast is the most unfavorable. The horizontal force between the mast and rollers P_z and axial force on the top of mast F can be obtained from the equilibrium condition of mechanics. Please see the reference [41] for the details.

The finite element analysis of a single-mast stacker crane is implemented programmatically using the ANSYS APDL language. Its purpose is to facilitate multiple finite element analysis in the topology optimization process.

C. STRENGTH ANALYSIS

The stacker crane is regarded as a bidirectional bending member. Its verifying calculation of strength is performed using the National Standard of China GB50017-2017 *Code for Design of Steel Structures* [43]. Basic allowable stress

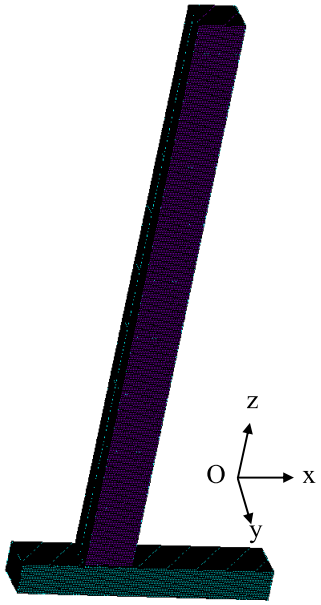

FIGURE 3. Finite element model of a stacker crane.

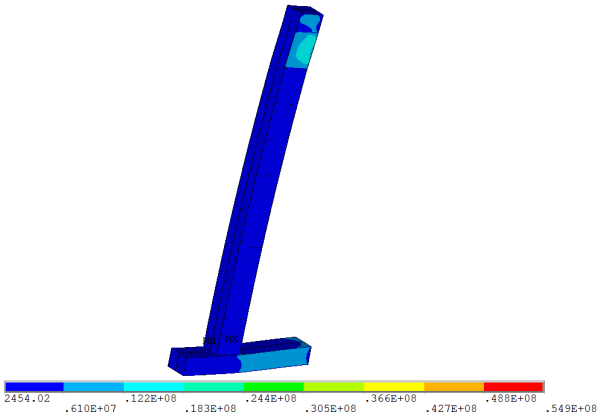

FIGURE 4. Equivalent stress cloud diagram of a stacker crane.

should be met as follows:

$$[\sigma] = 180MPa \tag{24}$$

The equivalent stress cloud diagram of a stacker crane is shown in Fig. 4. The maximum equivalent stress is 54.9 MPa, which appears at the junction of the bottom end rail and the mast. The maximum equivalent stress is less than the basic allowable stress, which meets the requirements for the strength of a stacker crane in the *Code for Design of Steel Structures*. The equivalent stress of the roller action area on the stacker crane is large, while other areas are in the low-stress area. This shows that the stacker crane has a large potential for weight reduction.

D. STATIC STIFFNESS ANALYSIS

There is no requirement for static stiffness of the bending member in the *Code for Design of Steel Structures*. There is no uniform standard for the static stiffness of a stacker crane. According to design experience, the allowable value of the

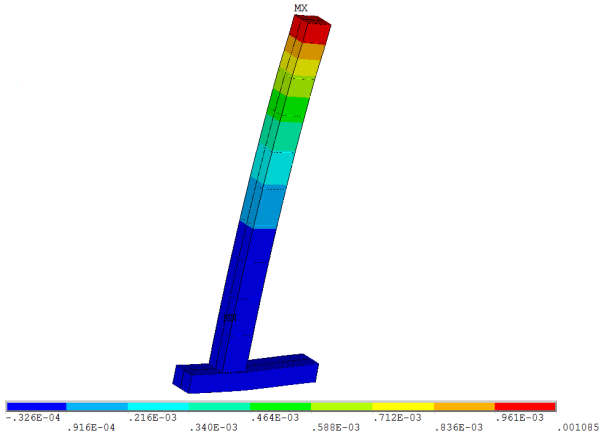

FIGURE 5. Displacement cloud diagram of a stacker crane along direction *x*.

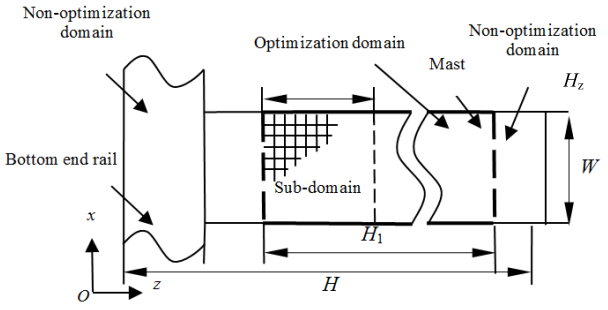

FIGURE 6. Optimization domain of a stacker crane.

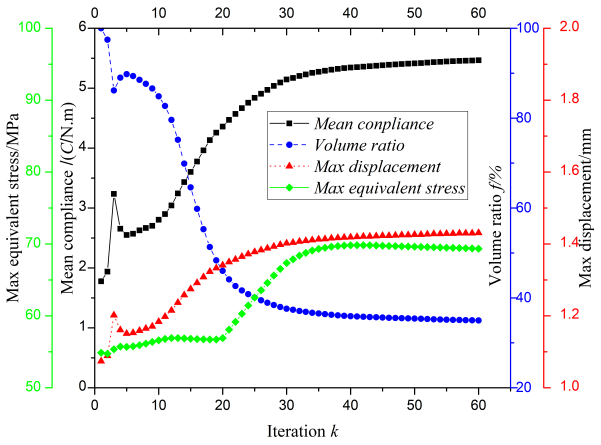

FIGURE 7. Optimization curve of mean compliance, volume ratio, maximum equivalent stress and maximum displacement along direction *x* for *m*=8.

static deflection $[f]$ usually satisfies the requirement as:

$$[f] = \frac{H}{2000} \sim \frac{H}{1000} = 4 \sim 8mm \tag{25}$$

The displacement cloud diagram of a stacker crane along direction x is shown in Fig. 5. The maximum displacement along direction x is 1.085 mm, which appears at the top of the mast. The maximum displacement is much smaller than the allowable static deflection, which meets the design's empirical requirements.

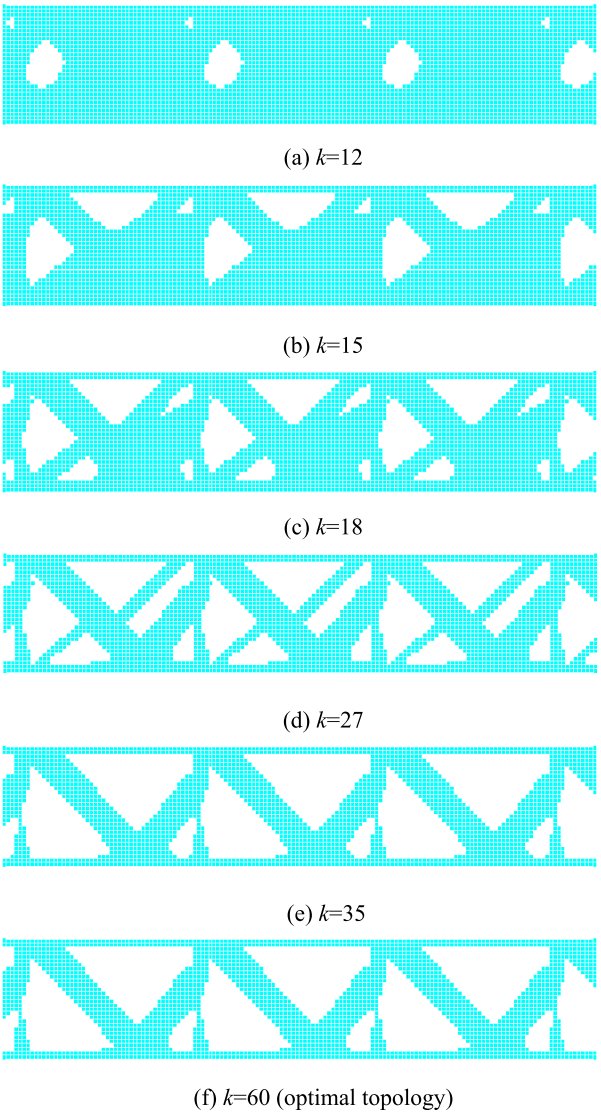

FIGURE 8. Process of periodic topology optimization for *m*=8.

VI. PERIODIC TOPOLOGY OPTIMIZATION OF A SINGLE-MAST STACKER CRANE

A. OPTIMIZATION DOMAIN AND PARAMETERS OF PERIODIC TOPOLOGY OPTIMIZATION FOR A STACKER CRANE

The optimization domain, with $H_1 = 7.2$ m and $W = 0.6$ m, is in the middle of the mast frontage, as shown in Fig. 6. The optimization domain is divided into $m = 6$, 8, 9 and 12 sub domains by partitions for $H_z = 1.2$ m, 0.9 m, 0.8 m and 0.6 m, respectively. The bottom end rail and other areas of the mast are non-optimization domains. Periodic topology optimization of the stacker crane is conducted based on the variable density method, in which elements' relative densities are selected as design variables and mean compliance is selected as the objective function under volume constraints. The modulus of elasticity of material and Poisson's ratio of material are $E_0 = 210$ GPa and $v = 0.3$. The penalization factor and volume ratio are $p = 3$ and $f = 35\%$, respectively.

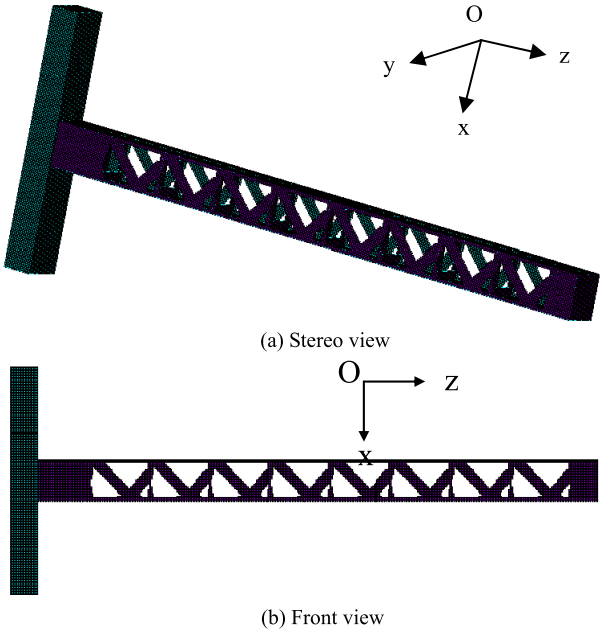

FIGURE 9. Optimal topology of a stacker crane for m=8.

The filtering radius and initial value of the design variable are $r_{\min} = 0.04$ m and $X^{(0)} = (1, 1, \cdots, 1)^{\mathrm{T}}_{m\times n}$.

B. PERIODIC TOPOLOGY OPTIMIZATION OF A STACKER CRANE FOR m=8

Fig. 7 shows the optimization curve of mean compliance C, volume ratio f, maximum equivalent stress and maximum displacement along direction x for $m = 8$. The mean compliance increases slowly as the volume ratio decreases stably. After 60 iterations, the volume ratio reaches 35%. Additionally, mean compliance varies from 1.777 N.m to 5.465 N.m. The maximum equivalent stress increases from 54.9 MPa to 69.3 MPa, and the maximum displacement along direction x ranges from 1.085 mm to 1.431 mm. The strength and static stiffness of the stacker crane still meet the requirements for the strength of a stacker crane in the *Code for Design of Steel Structures* and empirical design.

To distinctly express the process of periodic topology optimization, certain parts of the stacker crane are amplified. Fig. 8 shows the process of periodic topology optimization for $m = 8$, and Fig. 8f is the optimal periodic topology configuration. All elements with relative densities greater than 0.1 are displayed. Two holes appear simultaneously in each sub domain, which is a good period property. With the number of iterations increasing, some holes increase gradually or merge together. After the 35th iteration, the number of holes in each sub domain does not change, which means that the main body of optimal topology is forming. Until periodic topology optimization is complete, a similar trussed topology configuration is obtained, which has good periodicity. Fig. 8 shows the optimal topology of a stacker crane for $m = 8$, which is displayed entirely. Fig. 9a is the stereo view of the optimal topology, and Fig. 9b is the front view.

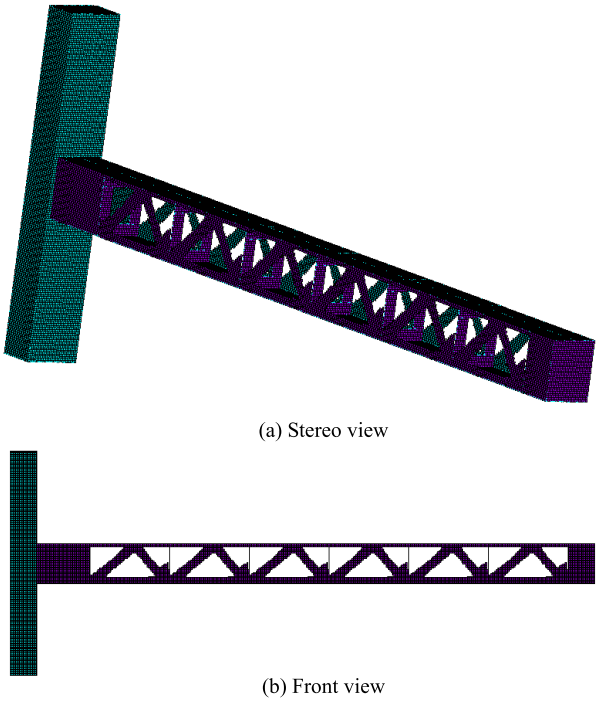

FIGURE 10. Optimal topology of a stacker crane for m=6.

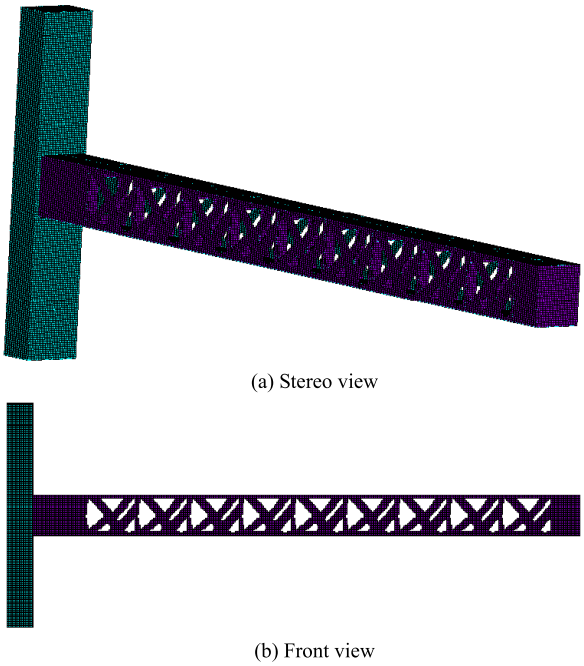

FIGURE 11. Optimal topology of a stacker crane for m=9.

The optimal topology is composed of eight upside-down '△' shapes, which satisfy the defined periodic conditions.

C. PERIODIC TOPOLOGY OPTIMIZATION OF A STACKER CRANE FOR m=6, 9, 12

Fig. 10, Fig. 11 and Fig. 12 show the optimal topologies of a stacker crane for $m = 6$, 9, and 12, respectively. The optimal topology for $m = 6$ is presented as six '△' shapes, which have

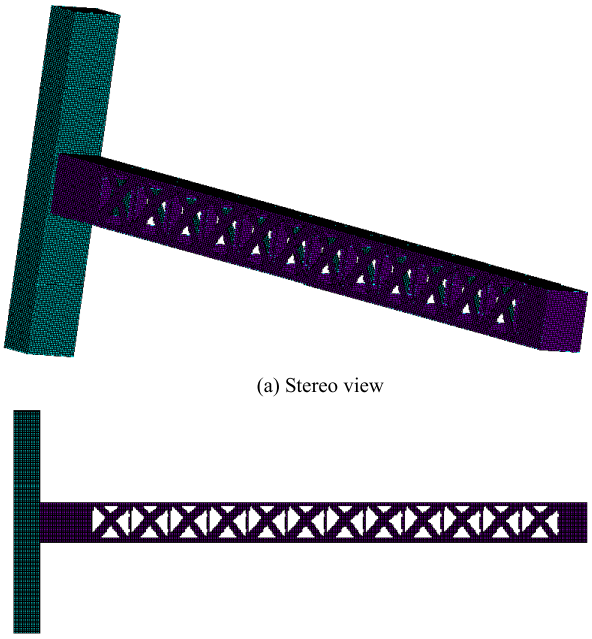

FIGURE 12. Optimal topology of a stacker crane for m=12.

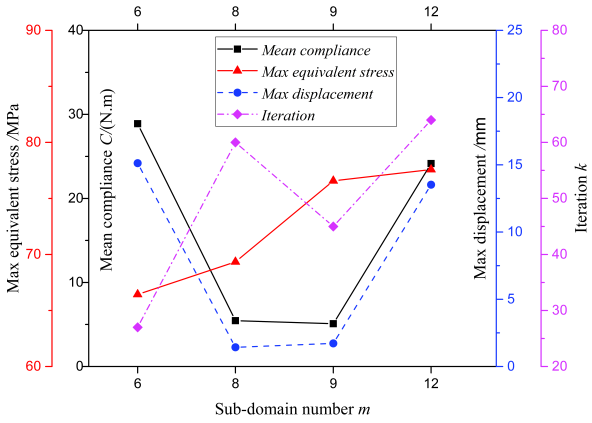

FIGURE 13. Curve of mean compliance, iteration number, maximum equivalent stress, and maximum displacement along direction x with sub domain number in the optimal topology.

a good period property. The optimal topology for $m = 9$ is more complicated than the optimal topology for $m = 6$ and 8. The optimal topology for $m = 12$ is composed of 12 'X' shapes. As the number of sub domains increases, different optimal topology configurations can be similarly obtained. This is mainly due to the change in the length-width ratio in the sub domain.

D. FINAL OPTIMAL TOPOLOGY OF A STACKER CRANE

Fig. 13 shows the curve of mean compliance C, iterations k, maximum equivalent stress and maximum displacement along direction x with the sub domain number in the optimal topology. When the sub domain numbers are 6 and 12, the maximum displacements along direction x are 15.12 mm and 13.52 mm, respectively, which do not satisfy the requirement for the static stiffness of a stacker crane.

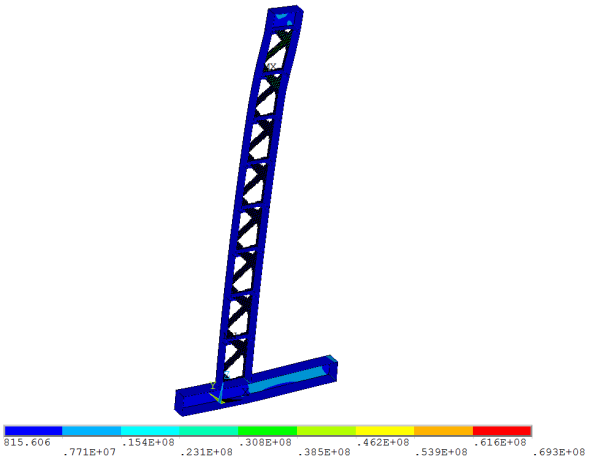

FIGURE 14. Equivalent stress cloud diagram of a stacker crane after optimization for m=8.

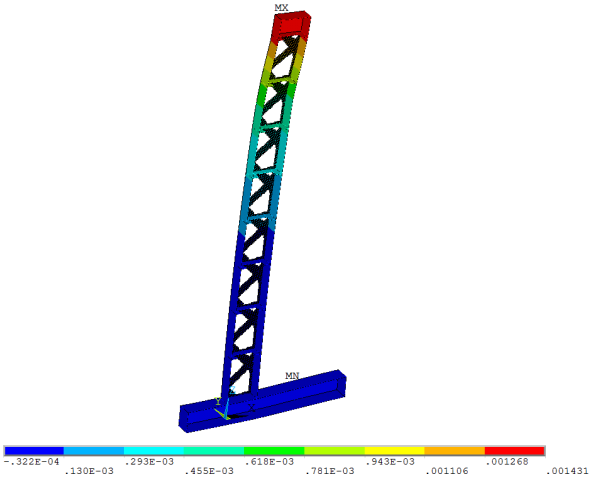

FIGURE 15. Displacement cloud diagram of a stacker crane along direction x after optimization for m=8.

The equivalent stress cloud diagram of a stacker crane after optimization for $m = 8$ is shown in Fig. 14. The maximum equivalent stress after optimization is 69.3 MPa. It is still smaller than the basic allowable stress, which meets the requirements for the strength of a stacker crane in the *Code for Design of Steel Structures*. The displacement cloud diagram of a stacker crane along direction x after optimization for $m = 8$ is shown in Fig. 15. The maximum displacement along direction x is 1.431 mm. It is still smaller than the allowable static deflection, which meets the design's empirical requirements. By considering mean compliance and the complexity of optimal topology configuration further, the optimal topology for $m = 8$ is the final optimal topology of periodic topology optimization for a stacker crane.

VII. LIGHTWEIGHT DESIGNS FOR THE STACKER CRANE

A preliminary lightweight design scheme is proposed based on the final optimal topology of the stacker crane, which is a periodic feature structure, as shown in Fig. 16.

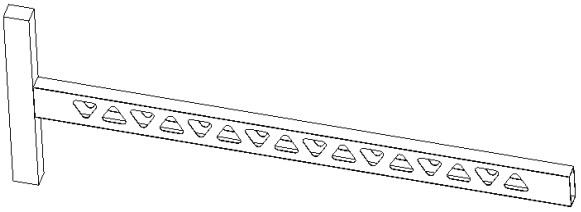

FIGURE 16. A preliminary lightweight design scheme for the stacker.

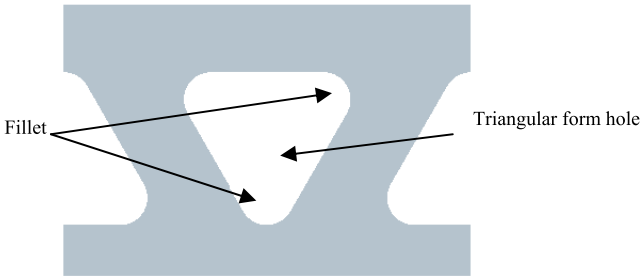

FIGURE 17. Process plan of sub domains.

The optimization domain is divided into eight by partitions. Each part has triangular form holes, and three corners of the hole are rounded off, as shown in Fig. 17.

VIII. CONCLUSION

In this paper, a method for periodic topology optimization of long-and-thin structures has been presented using the variable density method. The mathematical model of periodic topology optimization, in which elements' relative densities are selected as design variables and mean compliance as the objective function, has been established. An additional periodic constraint has been added to the mathematical model to ensure that the structure comprises a prescribed number of identical sub domains. The iterative formula of the virtual sub domain can be obtained based on the optimization criteria method.

To verify the capability and availability of the proposed method, periodic topology optimization of a single-mast stacker crane was investigated. The results show that a similar trussed topology configuration is obtained, which has good periodicity. As the number of sub domains increases, different optimal topology configurations with periodicity can be obtained likewise. This is mainly due to the change in the length-width ratio in the sub domain. By considering the mean compliance and complexity of the optimal topology configuration, the optimal topology for $m = 8$ is the final optimal topology of periodic topology optimization for the stacker crane.

A preliminary lightweight design scheme is proposed based on the final optimal topology of a stacker crane, which is a periodic feature structure.

REFERENCES

[1] N. Ryu, W. S. Song, Y. Jung, and S. Min, "Multi-objective topology optimization of a magnetic actuator using an adaptive weight and tunneling method," *IEEE Trans. Magn.*, vol. 55, no. 6, Jun. 2019, Art. no. 7202504.

[2] F. C. Potes, J. M. Silva, and P. V. Gamboa, "Development and characterization of a natural lightweight composite solution for aircraft structural applications," *Compos. Struct.*, vol. 136, no. 2, pp. 430–440, 2016.

[3] S. Doi, H. Sasaki, and H. Igarashi, "Multi-objective topology optimization of rotating machines using deep learning," *IEEE Trans. Magn.*, vol. 55, no. 6, Jun. 2019, Art. no. 7202605.

[4] M. Xia, S. Yang, and S. Ho, "A new topology optimization methodology based on constraint maximum-weight connected graph theorem," *IEEE Trans. Magn.*, vol. 54, no. 3, Mar. 2018, Art. no. 7001204.

[5] Y. Noguchi, T. Yamada, and S. Nishiwaki, "Topology optimization for hyperbolic acoustic metamaterials using a high-frequency homogenization method," *Comput. Methods Appl. Mech. Eng.*, vol. 335, pp. 419–471, Jun. 2018.

[6] G. Allaire, P. Geoffroy-Donders, and O. Pantz, "Topology optimization of modulated and oriented periodic microstructures by the homogenization method," *Comput. Math. Appl.*, vol. 78, no. 7, pp. 2197–2229, 2018.

[7] F. Zhao, "Topology optimization with meshless density variable approximations and BESO method," *Comput.-Aided Des.*, vol. 56, pp. 1–10, Nov. 2014.

[8] V. Kandemir, O. Dogan, and U. Yaman, "Topology optimization of 2.5 D parts using the SIMP method with a variable thickness approach," *Procedia Manuf.*, vol. 17, pp. 29–36, Jun. 2018.

[9] Y. Wang and Z. Kang, "A level set method for shape and topology optimization of coated structures," *Comput. Methods Appl. Mech. Eng.*, vol. 329, pp. 553–574, Feb. 2018.

[10] W. Khan and B. Ullah, "Structural optimization based on meshless element free Galerkin and level set methods," *Comput. Methods Appl. Mech. Eng.*, vol. 344, pp. 144–163, Feb. 2019.

[11] L. Xia, L. Zhang, Q. Xia, and T. Shi, "Stress-based topology optimization using bi-directional evolutionary structural optimization method," *Comput. Methods Appl. Mech. Eng.*, vol. 333, pp. 356–370, May 2018.

[12] L. Xia, Q. Xia, X. Huang, and Y. M. Xie, "Bi-directional evolutionary structural optimization on advanced structures and materials: A comprehensive review," *Arch. Comput. Methods Eng.*, vol. 25, no. 2, pp. 437–478, 2018.

[13] M. Y. Wang and S. Zhou, "Phase field: A variational method for structural topology optimization," *Comput. Model Eng. Sci.*, vol. 6, no. 6, pp. 547–566, Dec. 2004.

[14] A. Takezawa, S. Nishiwaki, and M. Kitamura, "Shape and topology optimization based on the phase field method and sensitivity analysis," *J. Comput. Phys.*, vol. 229, no. 7, pp. 2697–2718, Apr. 2010.

[15] Y. Sui, J. Du, and Y. Guo, "Independent continuous mapping for topological optimization of frame structures," *Acta Mech. Sinica*, vol. 22, p. 611, Dec. 2006.

[16] J. Du, Y. Guo, Z. Chen, and Y. Sui, "Topology optimization of continuum structures considering damage based on independent continuous mapping method," *Acta Mech. Sinica*, vol. 35, no. 2, pp. 433–444, Apr. 2019.

[17] J. Sokołowski and A. Żochowski, "On the topological derivative in shape optimization," *SIAM J. Control Optim.*, vol. 37, no. 4, pp. 1251–1272, 1999.

[18] F. Yuanfang, J. Dafeng, and Q. Weiwei, "Optimazation method for a mini electric vehicle frame structure," *J. Mech. Eng.*, vol. 45, no. 9, pp. 210–213, 2009.

[19] K. Lee, K. Ahn, and J. Yoo, "A novel P-norm correction method for lightweight topology optimization under maximum stress constraints," *Comput. Struct.*, vol. 171, pp. 18–30, Jul. 2016.

[20] Y. Chen, S. Zhou, and Q. Li, "Multiobjective topology optimization for finite periodic structures," *Comput. Struct.*, vol. 88, nos. 11–12, pp. 806–811, 2010.

[21] Z. H. Zuo, X. Huang, X. Yang, J. H. Rong, and Y. M. Xie, "Comparing optimal material microstructures with optimal periodic structures," *Comput. Mater. Sci.*, vol. 69, pp. 137–147, Mar. 2013.

[22] Y. Chen, P. Sareh, J. Feng, and Q. Sun, "A computational method for automated detection of engineering structures with cyclic symmetries," *Comput. Struct.*, vol. 191, pp. 153–164, Oct. 2017.

[23] Y. Tang, G. Dong, Q. Zhou, and Y. F. Zhao, "Lattice structure design and optimization with additive manufacturing constraints," *IEEE Trans. Autom. Sci. Eng.*, vol. 15, no. 4, pp. 1546–1562, Oct. 2018.

[24] B. Yi, Y. Zhou, G. H. Yoon, and K. Saitou, "Topology optimization of functionally-graded lattice structures with buckling constraints," *Comput. Methods Appl. Mech. Eng.*, vol. 354, pp. 593–619, Sep. 2019.

[25] M. Cui, X. Yang, Y. Zhang, C. Luo, and G. Li, "An asymptotically concentrated method for structural topology optimization based on the SIMLF interpolation," *Int. J. Numer. Methods Eng.*, vol. 115, no. 10, pp. 1175–1216, Sep. 2018.
[26] X. Huang and Y. M. Xie, "Optimal design of periodic structures using evolutionary topology optimization," *Struct. Multidisciplinary Optim.*, vol. 36, no. 6, pp. 597–606, 2008.
[27] T. Gao, W. H. Zhang, J. H. Zhu, and X. G. Tang, "Evolutionary static topology optimization of cyclic-symmetry structures," *Chin. J. Mech. Eng.*, vol. 44, no. 3, pp. 166–172, 2008.
[28] Z. H. Zuo, Y. M. Xie, and X. Huang, "Optimal topological design of periodic structures for natural frequencies," *J. Struct. Eng.*, vol. 137, no. 10, pp. 1229–1240, 2011.
[29] G. He, X. Huang, H. Wang, and G. Li, "Topology optimization of periodic structures using BESO based on unstructured design points," *Struct. Multidisciplinary Optim.*, vol. 53, no. 2, pp. 271–275, 2016.
[30] K. Long and J. Jia, "Periodic topology optimization design for thermal conductive structures using ICM method," *Eng. Mech.*, vol. 32, no. 5, pp. 227–235, 2015.
[31] J. Jia and K. Long, "Topology optimization for periodic thermal conductive material suing SIMP method," *J. Beijing Univ. Aeronaut. Astronaut.*, vol. 41, no. 6, pp. 1042–1048, 2015.
[32] A. Rietz, "Sufficiency of a finite exponent in SIMP (power law) methods," *Struct. Multidisciplinary Optim.*, vol. 21, no. 2, pp. 159–163, Apr. 2001.
[33] Y. Liang and G. Cheng, "Topology optimization via sequential integer programming and canonical relaxation algorithm," *Comput. Methods Appl. Mech. Eng.*, vol. 348, pp. 64–96, May 2019.
[34] R. Sivapuram and R. Picelli, "Topology optimization of binary structures using integer linear programming," *Finite Elements Anal. Des.*, vol. 139, pp. 49–61, Feb. 2018.
[35] K. C. Nguyen, P. Tran, and H. X. Nguyen, "Multi-material topology optimization for additive manufacturing using polytree-based adaptive polygonal finite elements," *Autom. Construct.*, vol. 99, pp. 79–90, Mar. 2019.
[36] Z. Chen, L. Gao, H. Qiu, and X. Shao, "Combining genetic algorithms with optimality criteria method for topology optimization," in *Proc. IEEE 4th Int. Conf. Bio-Inspired Comput.*, Oct. 2009, pp. 1–6.
[37] J. Ji, X. Ding, and M. Xiong, "Optimal stiffener layout of plate/shell structures by bionic growth method," *Comput. Struct.*, vol. 135, pp. 88–99, Feb. 2014.
[38] O. Sigmund and J. Petersson, "Numerical instabilities in topology optimization: A survey on procedures dealing with checkerboards, mesh-dependencies and local minima," *Struct. Optim.*, vol. 16, no. 1, pp. 68–75, Aug. 1998.
[39] X. Huang and Y. M. Xie, "Convergent and mesh-independent solutions for the bi-directional evolutionary structural optimization method," *Finite Elements Anal. Des.*, vol. 43, no. 14, pp. 1039–1049, 2007.
[40] J. Wang and Z. Zhang, *Crane Design Manual*. Beijing, China: China Raiway Press, 2013.
[41] Q. Zhou, "Calculation of metal structure of storage/retriveal machine," *Hoisting Conveying Machinery*, no. 5, pp. 3–6, 1992.
[42] A. Galkina and K. Schlacher, "Flatness-based model predictive control with linear programming for a single mast stacker crane," *IFAC-PapersOnLine*, vol. 51, no. 2, pp. 31–36, 2018.
[43] *Code for Design of Steel Structures*, Standard GB50017-2017, China Construction Press, Beijing, China, 2017.

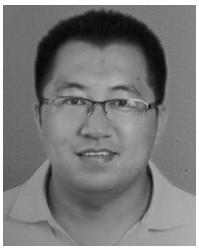

HONG-YU JIAO received the Ph.D. degree in mechatronic engineering from Tongji University, Shanghai, China, in 2015. He is currently a Postdoctoral with the Suzhou Institute of Nano-Tech and Nano-Bionics (SINANO), Chinese Academy of Sciences, Suzhou, China. His current research interests include optimization methods and optimal design of mechanical structure.

FENG LI received the Ph.D. degree in electrical engineering from the University of Cincinnati, USA, in 1999. He is currently a Research Professor with the Suzhou Institute of Nano-Tech and Nano-Bionics (SINANO), Chinese Academy of Sciences, Suzhou, China. His current research interests include micro nano photoelectron, nanomaterials, and nanomanufacturing.

ZHENG-YI JIANG, photograph and biography not available at the time of publication.

YING LI, photograph and biography not available at the time of publication.

ZHAO-PENG YU received the Ph.D. degree in material processing engineering from Jilin University, Changchun, China, in 2017. He is currently a Lecturer with the School of Automotive Engineering, Changshu Institute of Technology, Suzhou, China. His current research interests focus on optimization methods, functional material synthesis and applications, and biologically-inspired design methods.